J|A|C|S COMMUNICATIONS

Published on Web 01/06/2009

Method to Derive Restoring Forces of Strained Molecules from Kinetic Measurements

Zhen Huang, Qing-Zheng Yang, Daria Khvostichenko, Timothy J. Kucharski, Joseph Chen, and Roman Boulatov*

Department of Chemistry, University of Illinois, Urbana, Illinois 61801

Received September 8, 2008; E-mail: Boulatov@uiuc.edu

We propose a method to quantify the restoring force of a constrained small molecule and relate its reactivity to this force. The method bridges the studies of macromolecular reactions in force spectroscopies[1] with those of corresponding strained monomers and is essential for rational design of molecular actuators.[2] We illustrate our method by showing that *E* stiff stilbene (1,1′-Δ-biindan, Figure 1) with up to ∼700 pN of force along its C6,C6′ axis is accessible by photoisomerization with the quantum yield and thermal stability depending strongly on the restoring force.

The capacity of living organisms to convert conformational changes in a reacting molecule into directional motion has stimulated considerable effort to understand the underlying principles[3,4] and to realize them in synthetic systems.[2] The simplest, paradigmatic example is a single molecule of *E*-oligoazobenzene stretched between an AFM tip and a glass slide.[5] Its contraction on irradiation brings the tip closer to the slide by bending the AFM cantilever. Here the macromolecule is constrained along a single axis into a nonequilibrium configuration which creates a gradient of the molecular free energy (restoring force) along this axis. This restoring force is balanced by the elastic force of the bent cantilever. Irradiation-induced contraction of the oligomer along the constrained axis suggests an increase in the restoring force upon electronic excitation of azobenzene and is consistent with the current understanding of the topologies of the ground and excited-state surfaces of free azobenzene. Of outstanding contemporary interest is how these surfaces are perturbed by the constraint, that is, how the quantum yields of *E*→*Z* photoisomerization and activation energies of thermal isomerizations depend on the restoring force. For example, it imposes a fundamental limit on the actuation capacity of the oligomer and the energy conversion efficiency.

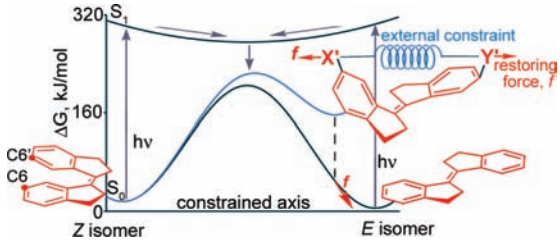

Figure 1. Qualitative representation of the energy surface of stiff stilbene along the C6,C6′ axis. On the S_0 surface, the two isomers are separated by a >170 kJ/mol barrier making photoisomerization, which requires electronic excitation to S_1, the only important isomerization mechanism. Constraining stiff stilbene along its C6,C6′ molecular axis either by a macroscopic object such as AFM or a molecular fragment perturbs the S_0 surface and generates a restoring force (energy gradient along the constrained axis). A compressive constrain (shown) decreases the quantum yield of *Z*→*E* and the activation energy of thermal *E*→*Z* isomerizations. These effects limit the maximum force obtainable from stiff stilbene. Perturbation of the S_1 surface by the constraints is not shown.

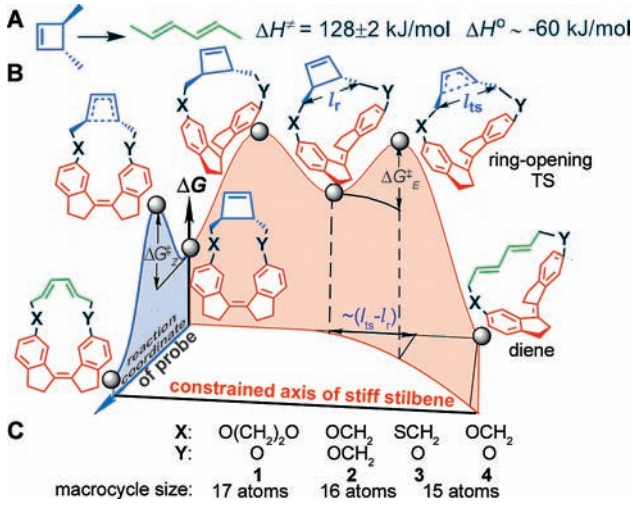

Figure 2. (A) The molecular force probe. (B) The energy diagram underlying the use of cyclobutene as a molecular force probe: the inert linkers X and Y make the reaction coordinate of the probe orthogonal to the C6−C6′ axis of relaxed *Z* stiff stilbene but constrain *E* stiff stilbene and align its C6−C6′ axis with the $CH_2\cdots CH_2$ axis of the probe. The elongation of the probe during its reaction is equivalent to partial relaxation of the constraint, which lowers the barrier of the probe reaction, $\Delta G^{\ddagger}_E < \Delta G^{\ddagger}_Z$. (C) Compositions of the linkers, size and number of macrocycles described. Atom on the right is bound to stiff stilbene.

Although single-molecule force experiments showed suppression of photoisomerization at forces >400 pN they cannot yet reveal the molecular basis of this suppression. In such experiments, neither the quantum yields nor activation barriers can yet be measured and the fraction of monomers in the *E* or *Z* configuration can only be inferred indirectly. Such macromolecular systems remain too large for quantum chemical modeling. The contraction of oligoazobenzene is most likely stepwise, with a rare but rapid (∼ps)[6] conformational transition in each monomer occurring independent of the other monomers and generating a localized structural change that is comparable or smaller than average thermal fluctuation. Hence, the effect of external load on conformational transitions of an oligomer is related closely to the kinetics of an isolated monomer constrained to the same restoring force along the appropriate molecular axis.

Here we show that a molecular force probe instead of a macroscopic one, such as AFM, can be used both to constrain a small molecule (substrate) along a single axis and to estimate the resultant restoring force. This molecular force probe is a small reactant whose thermally accessible transition state allows a partial relaxation of the constrained substrate primarily along a single axis (Figure 2). This relaxation lowers the energy of the transition state of the probe relative to that of the probe connected to an unconstrained substrate. The difference, $\Delta\Delta G^{\ddagger}$ is measured. The

geometries of the substrate constrained by the probe in its ground and transition states are calculated quantum-chemically and validated against experimental $\Delta G^{\ddagger}$. The ratio of measured $\Delta\Delta G^{\ddagger}$ to the calculated elongation of the force probe along the constrained axis, $\Delta l = l_{ts} - l_r$ (Figure 2B), gives the upper limit of the average restoring force in the substrate constrained by the probe in its ground and transition-state conformations. The low limit is estimated by calculating the fraction of $\Delta\Delta G^{\ddagger}$ due to relaxation of the probe and/or the substrate orthogonal to the constrained axis.

Although kinetic effects of molecular strain have been extensively studied,[7] no quantitative relationships between rates and restoring forces exist. Known strained small molecules poorly mimic the axial strain generated in force spectroscopies or during microscopic actuation. In the absence of a single constrained molecular axis, restoring force is not a useful quantifier of molecular strain, thus requiring the use of scalar strain energy.

These limitations are overcome with thermal ring-opening of *trans*-3,4-dimethylcyclobutene to *trans*,*trans*-hexadiene (Figure 2), which uniquely satisfies the criteria of an ideal molecular force probe. First, since the method is predicated on accurately calculating the transition state of the probe, mechanistically simple solvent-independent unimolecular rearrangements of small reactants of second row elements are preferred. Second, structurally anisotropic probes that undergo structural changes primarily along a single molecular axis minimize distortions of the substrate along other axes. Third, the probe should be easy to connect to the substrate through the atoms that define this axis. Fourth, the probe along this axis should be much stiffer than the substrate along its constrained axis. Otherwise, distortions of the probe could affect its kinetics obscuring barrier lowering due to the substrate relaxation. Fifth, practically irreversible probe reactions allow the restoring force of even highly thermally labile constrained substrates to be measured, as illustrated below for compound **2** (Figure 2C). Finally, optically transparent probes permit restoring forces generated in photoisomerizations to be quantified.

We illustrate this approach by estimating the maximum accessible restoring force along the C6,C6′ axis of stiff stilbene (Figure 1). Like azobenzene, stiff stilbene undergoes facile $E \rightarrow Z$ photoisomerization at 375 nm.[8] The activation energy of thermal $Z \rightarrow E$ isomerization of stiff stilbene is ~60 kJ/mol higher than that of azobenzene; combined with its greater conformational rigidity much higher restoring forces are accessible in stiff stilbene. Stiff stilbene derivatization is most convenient at the C6,C6′ positions making constraints along this axis most relevant for the development of new actuators.

In this study we used macrocycles **1**−**4** (Figure 2), which differ in the number of atoms linking the C6,C6′ atoms. By gradually decreasing their length, the *E* isomer is increasingly constrained. We synthesized the *Z* isomers of **1**−**4** in 7−9 steps and 5−15% overall yields from racemic *trans*-3,4-bis(hydroxylmethyl)cyclobutene and C6-substituted indanones (Supporting Information, Figure S1). Macrocyclization, affected in the final step in 50−80% yield by McMurry coupling,[9] produced exclusively *Z* isomers. This high yield and stereoselectivity illustrate the conformational rigidity of stiff stilbene, which decreases the entropic cost of macrocyclization and destabilizes the *E* isomer. All compounds were characterized by ^{1}H NMR, UV−vis and high-resolution mass spectroscopies, and the chemical homogeneity was verified by HPLC.

Heating the *Z* macrocycles in the dark at 370−415 K resulted in clean conversion of the probe to the diene form (Figure 2). The reactions were followed by ^{1}H NMR and HPLC. The corresponding Arrhenius plots (Figure S6) were linear and yielded the activation enthalpies (Table 1) similar to that for free *trans*-3,4-dimethylcyclobutene, indicating negligible perturbation of the probe by *Z* stiff stilbene. The activation entropies, $\Delta S^{\ddagger}$, were small and insensitive to the size of the macrocycle (Table S6).

Table 1. Measured and Calculated Activation Enthalpies of the Probe Reaction (300 K), Calculated Boltzmann-Weighted Average Elongation of the Force Probe in the Ring-Opening Transition State, $\langle\Delta l\rangle$, and the Restoring Force of *E* Stiff Stilbene in **1**−**4**.

	1	**2**	**3**	**4**
$\Delta H^{\ddagger}_Z$, kJ/mol (exptl)	124 ± 2	126 ± 2	126 ± 2	120 ± 2
$\Delta H^{\ddagger}_Z$, kJ/mol (calcd)	124	128	124	120
$\Delta H^{\ddagger}_E$, kJ/mol (exptl)	101 ± 3	89 ± 3		
$\Delta H^{\ddagger}_E$, kJ/mol (calcd)	100	92	92	90
$\Delta\Delta H^{\ddagger}$, kJ/mol	23 ± 4	37 ± 4	34 ± 2	30 ± 2
$\Delta\Delta H_{\perp}^{\ddagger}$, kJ/mol (calcd)	7	1	6	14
$\langle\Delta l\rangle$, Å (calcd)	0.725	0.751	0.728	0.712
$\langle f\rangle^{high}$, pN	520 ± 20	800 ± 40	760 ± 40	680 ± 50
$\langle f\rangle^{low}$, pN	370 ± 20	780 ± 40	620 ± 40	350 ± 50
$\langle f\rangle^{SCF}$, pN	430	510	450	540
av of 3 estimates, pN	440	690	610	520

Irradiation of the largest macrocycle **1** at 375 nm generated a photostationary state containing 9% (mol) of *E*-**1**, with the quantum yield, $\varphi_{Z\rightarrow E} = 0.17 \pm 0.09$, $^1/_3$ that in free stiff stilbene (0.5). Heating *E*-**1** at 305−333 K in the dark resulted in the clean probe reaction with $\Delta H^{\ddagger}_E = 101 \pm 3$ kJ/mol (23 ± 5 kJ/mol lower than *Z*-**1**, Table 1); thermal relaxation of *E*-**1** to *Z*-**1** was negligible.

The fractions of the *E* isomers at the photostationary states of smaller macrocycles **2**−**4** were below our detection limit (<1%). However, continuous irradiation of dilute heptane solutions of *Z*-**2** (total absorbance <0.1) at 325−363 K accelerated the probe reaction up to 10^3-fold compared to that in *Z*-**2** in the dark. The temperature and photon-flux dependence of the overall rate, $v_{Z\text{-}2}$, was consistent with the mechanism in Figure 3 and the corresponding rate law, eq 1, derived for the steady-state approximation in *E*-**2**. Using this rate law we obtained the activation enthalpies of the probe reaction ($\Delta H^{\ddagger}_E$) and of thermal *E*-**2**→*Z*-**2** relaxation ($\Delta H^{\ddagger}_{E\rightarrow Z}$) from measured $v_{Z\text{-}2}$ (Figure 4). The former decreased by >35 kJ/mol relative to *Z*-**2** and the latter by ~100 kJ/mol (to 69 ± 4 kJ/mol) relative to free stiff stilbene. Consequently, the primary thermal reaction of *E*-**2** was relaxation to *Z*-**2** ($\tau_{1/2} \approx 100$ ms vs 17 days for *E*-**1** and ≈10^9 years for free stiff stilbene at 300 K). The rates however, remain too slow to compete with vibrational relaxation of stiff stilbene ($\tau_{1/2}$ < 100 ps[5]), suggesting that nonthermalized macrocycles contribute negligibly to the rates.

We estimated the quantum yield of generating *E*-**2**,$\varphi_{Z\rightarrow E}$ from the intercept of the semilog plot in Figure 4B assuming that (i) $(\varphi_{E\rightarrow Z}\epsilon_{E\text{-}2})/(\varphi_{Z\rightarrow E}\epsilon_{Z\text{-}2})$ is temperature-independent (since the plots in Figure 4A are linear); (ii) $\epsilon_{Z\text{-}2}/\epsilon_{E\text{-}2} \approx \epsilon_{Z\text{-}1}/\epsilon_{E\text{-}1}$ (since spectra of *Z*-**1** and *Z*-**2** are nearly identical, Figure S3); (iii) $\Delta S^{\ddagger}_{E\text{-}2} \approx \Delta S^{\ddagger}_{E\text{-}1}$ (since $\Delta S^{\ddagger}$ is similar in all *Z* isomers and *E*-**1**). The fluorescence

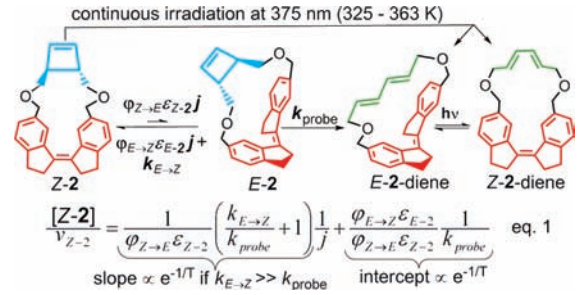

Figure 3. The mechanism responsible for up to 10^3-fold acceleration of the probe reaction upon irradiation of *Z*-**2** and the corresponding rate law: [*Z*-**2**] is the concentration of *Z*-**2**, $\varepsilon_{Z\text{-}2}$ and $\varepsilon_{E\text{-}2}$ are molar absorptivities of *Z*-**2** and *E*-**2** and *j* is the incident photon flux density.

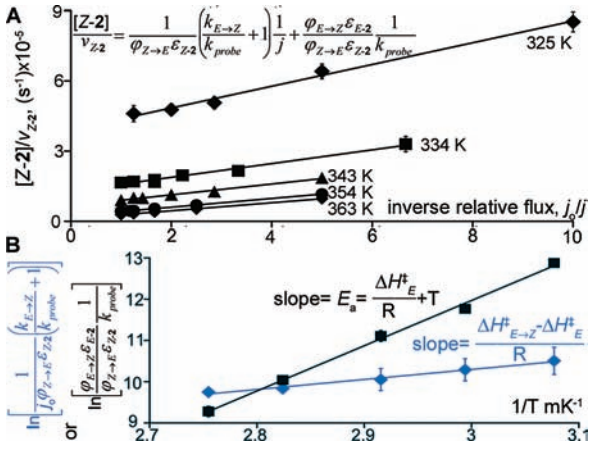

Figure 4. (A) The dependence of the depletion rate of *Z*-**2** under continuous irradiation, v_Z, follows eq 1 (shown) at multiple temperature and photon fluxes; $j_o = 10^{18}$ photons/(s cm^2). (B) Arrhenius plots of the slopes (blue) and intercepts of the linear least-squares fits (solid lines) from panel A. Errors of some points are smaller than the symbols.

quantum yield in *Z*-**2** is <0.05, suggesting that $\varphi_{E\to Z} \approx 1$ and hence $\varphi_{Z\to E} \approx 10^{-3}$. The quantum yield of forming *E*-**2** is lowered ~1000 fold from that of free stiff stilbene by the imposed constraint.

The probe reaction was not accelerated upon irradiation of the smallest macrocycles *Z*-**3** and *Z*-**4**. Since the expected products, *E*-**3**-diene and *E*-**4**-diene, prepared independently, were stable, *E* stiff stilbene in *E*-**3** and *E*-**4** must be inaccessible.

To obtain the restoring force of *E* stiff stilbene in **1**−**4** we optimized all conformers of the ground and ring-opening transition states in both isomers of **1**−**4** at the O3LYP/6-311G(2d,p) level of the DFT.[10] For all six compounds with the available experimental activation enthalpies, the difference between the calculated and experimental values was within the experimental uncertainty (2−3 kJ/mol, Table 1), lending credence to the calculated structures and $\Delta H^{\ddagger}_E$ for *E*-**3** and *E*-**4**, which are not available experimentally.

We estimated the high limit of the restoring force of stiff stilbene in macrocycles **1**−**4** by assuming that $\Delta\Delta G^{\ddagger}$ (~$\Delta\Delta H^{\ddagger}$) arises solely from the relaxation along the C6,C6′ axis. Out of several internuclear distances parallel to the C6,C6′ axis of stiff stilbene we used the separation of the methylene carbons closest to the C_4H_4 core (Figure 2B). Its elongation in the transition state reflects conformational relaxation of both stiff stilbene and the linkers and hence exceeds the changes in the separation of the C6,C6′ carbons. The internal mechanical equilibrium in a macrocycle ensures that the restoring force at the methylene carbons equal that at the C6,C6′ carbons. We used the Boltzmann-weighted average separation of the CH_2 groups in all respective conformers.

To estimate the low limit of the restoring force of stiff stilbene in the *E* isomers of **1**−**4**, $\langle f \rangle^{\text{low}}$, we optimized all conformers of *trans*-(*cyclo*-C_4H_4)(CH_2OCH_3)$_2$ (and the corresponding thio derivatives for **4**) in the ground and ring-opening transition states and identified those conformers that best reproduced the structures of these moieties in the macrocycles. We assumed that the enthalpy difference between the best-match and minimum-energy conformers of *trans*-(*cyclo*-C_4H_4)(CH_2OCH_3)$_2$ quantifies all strain orthogonal to C6,C6′ axis. Table 1 lists the barrier-lowering due to relaxation of this strain, $\Delta\Delta H_{\perp}^{\ddagger}$ and $\langle f \rangle^{\text{low}} \approx (\Delta\Delta H^{\ddagger} - \Delta\Delta H_{\perp}^{\ddagger})/\Delta l$.

We also calculated the vectoral sum of atomic forces in fragments obtained by excising the C_4H_4 core from each macrocycle and adding H atoms to the newly terminal CH_2 groups. In macrocycles the restoring force of strained stiff stilbene is balanced by that of the force probe and excising the latter results in uncompensated forces on each nucleus of the remaining fragment. We calculated these atomic forces as analytical gradients of the electronic energy of a fragment at its geometry in the full macrocycle for all conformers of both isomers of **1**−**4** in the ground and ring-opening transition states. Table 1 lists the difference in the total atomic forces in *E* and *Z* isomers of each macrocycle projected on the C6,C6′ axis and averaged between the ground and transition state conformers, $\langle f \rangle^{\text{SCF}}$.

Forces estimated by the three methods are in reasonable agreement. Importantly, comparable forces are obtained *without* knowing the geometries of the macrocycles, using instead the elongation of the CH_3-CH_3 separation in free *trans*-3,4-dimethylcyclobutene (0.754 Å). On the other hand, the data suggest the restoring force at the equilibrium geometry alone to be insufficient to predict quantitatively the kinetics in the presence of constraints: preliminary calculations suggest that inaccessibility of *E*-**3** may be due to its greater restoring force in the transition state (and probably conical intersection) of *E*→*Z* isomerization relative to *E*-**2**, although the opposite is true in their ground states.

At least 10^2-fold higher force is required to suppress the isomerization of stiff stilbene than to stall a motor protein, e.g., myosin.[3,4] These proteins generate force *orthogonal* to their ~100-nm long coil−coil stalks,[3] whose flexural rigidity is far lower than the linear stiffness of a macromolecule *along* its end-to-end axis. Unlike isomerization of stiff stilbene, the kinetics of ATP hydrolysis is very sensitive to small distortions of the catalytic site,[3] which allows many motor proteins to slow down the ATPase activity as the restoring force increases and approach unit energy coupling efficiency at the stall force.[3,4] In contrast, molar absorptivity of stiff stilbene varies little with its restoring force (Table S3) and as the quantum yield of *Z*→*E* photoisomerization drops precipitously with force, the fraction of absorbed photon energy dissipated as heat increases rapidly. Approximating useful work in **1**−**4** with $\Delta\Delta G^{\ddagger}$, the coupling efficiency of stiff stilbene decreases from 6% at ~500 pN (*E*-**1**) to 0.03% at ~700 pN (*E*-**2**).

Unlike strain energy, restoring force is a size-invariant measure of molecular strain. While defined unambiguously in the multidimensional configuration space, to be broadly useful restoring force needs to be expressed as a Cartesian vector. The method reported here should help address some of the many conceptual and technical ambiguities of doing so.[4,11]

Acknowledgment. The work was supported by the NSF, US Air Force Office of Scientific Research, the donors of the PRF, and the University of Illinois. T.K. thanks the ONR and NSF for predoctoral fellowships. The HPCMP program of the DoD and NSF NCSA provided grants of computational time.

Supporting Information Available: Details of synthetic procedures, kinetic measurements, computational protocols, and spectroscopic characterization of **1**−**4**. This material is available free of charge via the Internet at http://pubs.acs.org.

References

(1) Neuman, K. C.; Nagy, A. *Nat. Methods* **2008**, *5*, 491.
(2) Browne, W. R.; Feringa, B. L. *Nat. Nanotechnol.* **2006**, *1*, 25.
(3) Schliwa, M. *Molecular Motors;* Wiley: New York, 2003.
(4) Reimann, P. *Phys. Rep.* **2002**, *361*, 57.
(5) Hugel, T.; Holland, N. B.; Cattani, A.; Moroder, L.; Seitz, M.; Gaub, H. E. *Science* **2002**, *296*, 1103.
(6) Sension, R. J.; Repinec, S. T.; Hochstrasser, R. M. *J. Chem. Phys.* **1990**, *93*, 9185.
(7) Cremer, D.; Kraka, E. In *Molecular Structure and Energetics*; Liebman, J. F., Greenberg, A., Eds.; VCH: New York, 1988; Vol. 7, pp 65−138.
(8) Improta, R.; Santoro, F. *J. Phys. Chem. A* **2005**, *109*, 10058.
(9) McMurry, J. E. *Chem. Rev.* **1989**, *89*, 1513.
(10) We established the stability of all converged SCF wave functions.
(11) Changbong, H.; Thirumalai, D. *J. Phys.: Cond. Matter* **2007**, 113101–1.

JA807113M